

Selective Visualization Techniques for Surface and Microstructure of Steel Products by Scanning Electron Microscopy[†]

AOYAMA Tomohiro^{*1} NAGOSHI Masayasu^{*2} SATO Kaoru^{*3}

Abstract:

JFE Steel has developed observation techniques utilizing scanning electron microscopy (SEM) and their application to steel products. An appropriate selection of SEM conditions and detectors achieves selective imaging of surface information such as the chemical state, topography, mean atomic number and crystallography. Elemental analyses under low primary electron energy improve spatial resolution and also enable characterization of chemical states. A combination of these techniques improves understanding of the relationship between the microstructures and important properties of steel products and can serve as a lodestar for the design and development of novel materials.

1. Introduction

Steel materials are used in a variety of applications, as exemplified by automobiles, electrical appliances and ships, among others. In addition to mechanical properties such as strength and ductility, various other properties are also required in steel materials. These include paintability, coatability, external appearance, sliding properties during forming, etc. In developing steel products with superior properties, it is important to understand the steel microstructure and surface morphology, which contribute to these properties, in a wide range of scales from a few nanometers (nm) to a few 100 micrometers (μm).

Scanning electron microscopy (SEM) is one funda-

mental material characterization technique. SEM is also widely used for steel materials, as it has a number of advantages including a wide observational magnification range, deep focal depth and comparatively easy sample preparation, and it is also possible to add functions such as elemental analysis by a characteristic X-ray analysis and crystallographic analysis by an electron backscatter pattern (EBSP) measurement. The prototype of the SEM which obtains images by scanning an electron beam was created in 1935¹⁾. The most of existing fundamental SEM technologies were established from the 1950s through the beginning of the 1960s²⁾ and were commercialized in 1965³⁾. Subsequently, the performance and convenience of SEM was greatly enhanced thanks to a diverse range of technical innovations and improvements such as improvement of the field emission electron gun and objective lens, introduction of personal computer control techniques, etc. Recent years have also seen dramatic improvements in SEM technology with the development of ultra-low accelerating voltage SEM (ULV-SEM), which improves effective spatial resolution and surface sensitivity by irradiation of primary electron with ultra-low energy (≤ 1 keV), and selective visualization techniques for various types of sample information by using multiple detectors. On the other hand, the interpretation of SEM images has become even more complex, and this has heightened the importance of contrast interpretation based on experiments and calculations.

JFE Steel recognized the usefulness of ULV-SEM

[†] Originally published in *JFE GIHO* No. 37 (Feb. 2016), p. 16–22



^{*1} Dr. Eng.,
Senior Researcher Deputy Manager,
Analysis & Characterization Research Dept.,
Steel Res. Lab.,
JFE Steel



^{*2} Ph. D.,
General Manager,
Analysis & Characterization Research Dept.,
Steel Res. Lab.,
JFE Steel



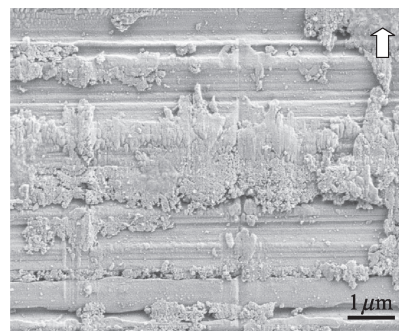
^{*3} Ph. D.,
Fellow,
Corporate Planning Dept.,
JFE Techno-Research

instantaneously. After introducing ULV-SEM in 2001, the company grappled with the development of top surface observation techniques for steel materials⁴⁻¹⁴. “Special Issue on Analytical Sciences and Microstructural Characterization” (Japanese edition of JFE Technical Report) in 2006 introduced ULV-SEM technology and reported its advantages⁶. The present report introduces the results of study of selective visualization techniques for secondary electron (SE) and backscattered electron (BSE) information. In addition, JFE’s efforts in connection with elemental analysis techniques utilizing low accelerating voltages (LV) are also presented. It should be noted that the experiments in the examples presented herein were performed with a Schottky type SEM made by LEO Elektronenmikroskopie GmbH (now Carl Zeiss Microscopy GmbH) or Carl Zeiss Microscopy GmbH equipped with hybrid objective lenses combining electrostatic and magnetic field lenses.

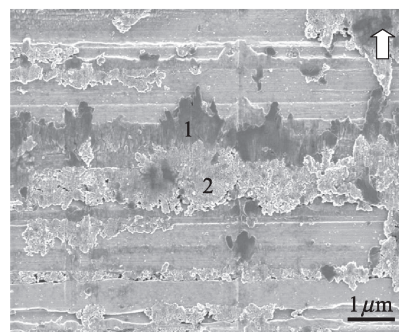
2. Selective Visualization of SE Information

Secondary electron (SE) emission occurs when primary electrons that have penetrated a specimen diffuse while losing energy. That energy is low, only a few 10 electron volts (eV) or less, and the amount of emission from the specimen surface is easily affected by the surface state of the specimen such as surface topography, differences in material, electrical charge, and so on. JFE Steel established a technology for selective visualization of surface information by selecting the range of SE energy which is to be detected preferentially under a low primary electron energy (E_p) condition by appropriate selection of the type and arrangement of detectors.

Photo 1¹¹⁾ shows SEM images of the same field of view of the tool surface after a sliding test which was conducted to elucidate the sliding mechanism of galvanized (GA) steel sheets. The images were observed at $E_p=1$ keV with an Everhart-Thornley detector (E-T detector) equipped in the SEM chamber and an inlens-SE detector equipped in the column. In Photo 1 (a), which was taken with the E-T detector, topographic information is emphasized, and the shape of the substance adhering to the tool surface can be observed. In Photo 1 (b), which was taken with the inlens-SE detector, material information is emphasized. From the difference in contrast, it is clear that the adhering substance consists of two kinds of substances, as indicated by 1 and 2. The results of transmission electron microscope (TEM) observation revealed that adhering substance 1 is a dense composite layer which consists of an Al oxide and Fe-Zn alloy and has adhered firmly to the convex part of the tool surface; this substance is considered to resemble the so-called built-up edge that forms on the surface of cutting tools¹¹⁾. On the other hand, adhering substance 2



(a) By Everhart-Thornley (E-T) detector



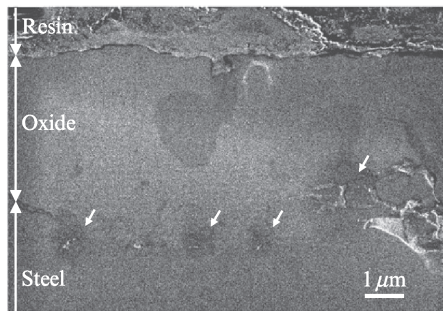
(b) By in-lens secondary electron (SE) detector
Arrows indicate the sliding direction of the steel sheet.

Photo 1 Plan view secondary electron (SE) images of the tool surface after a sliding test of a galvanized (GA) steel sheet¹¹⁾ (The primary energy of incident electron (E_p) was 1 keV from the same area.)

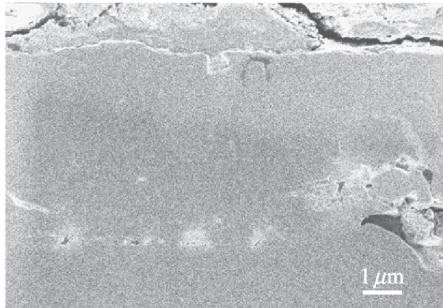
is an Fe-Zn alloy. It is not completely bonded to the tool surface and is considered to be part of the GA coating layer which was plowed up by adhering substance 1¹¹⁾. Based on these results, a new mechanism of adherence of GA and the tool surface was proposed. This trial is expected to provide a surface design of a steel sheet with a higher lubricity.

Among the SE emitted from specimens, the inlens-SE detector of the SEM instrument used in the actual example in Photo 1 (a) is designed to enable high efficiency detection of SE mainly in the low energy region. The fact that the inlens-SE detector is sensitive to differences in materials is thought to be because it is easily affected by changes in the material work function and surface potential due to local charge. In contrast, the E-T detector detects a low percentage of low energy SE that are sensitive to the material state and also emphasizes the surface topography by a projection effect, which is due to the arrangement of the detector at a position obliquely above the specimen. This difference in the features of these detectors has also been confirmed by the calculation of electron orbit, etc.¹⁵⁾.

In order to understand the mechanism of SE information selectivity empirically, the energy region of the electrons that contribute to contrast formation with these devices was investigated by using an inlens detector



(a) Filtering energy: 0–30 eV



(b) Filtering energy: 100–300 eV

Photo 2 Subtracted images of energy filtered scanning electron microscopy (SEM) images of the cross-section of thermally-oxidized carbon steel¹⁶⁾ (The images were obtained by subtracting the image intensities of different filtering voltages from the same area. The primary energy of incident electron (E_p) was 1.5 keV)

with an energy filter¹⁰⁾. SEM images of the same field of view of the cross section of a carbon steel specimen, which had been heat-treated to form an oxide layer on the surface, were taken at different filter voltages, and subtraction images were obtained by performing arithmetic image processing on these SEM images. These subtraction images selectively incorporate SE of a certain energy range. **Photo 2**¹⁶⁾ shows the SEM subtraction images obtained by the procedure outlined above. Photo 2 (a) is the subtraction image for the energy range from 0 to 30 eV, and Photo 2 (b) is the image for the range from 100 to 300 eV. The dark contrast shown by the white arrows in Photo 2 (a) is caused by the charge of the abrasive, which was adsorbed during cross-sectional sample preparation. In Photo 2 (b), which includes electrons in a higher energy region, the contrast caused by this charge largely vanished, and the crack shape became clear. From these results, it is considered to be possible to obtain images which emphasize material information by SE in the low energy region, and images which emphasize topographic information by SE in the higher energy region¹⁰⁾.

Thus, understanding of the mechanism of formation of SE contrasts facilitates interpreting information from observed SE images correctly, and thereby clarify the specimen structure and morphology. It is also possible

to obtain surface information selectively for properties of interest, and as a result, useful knowledge for the design and development of new steel products can be obtained.

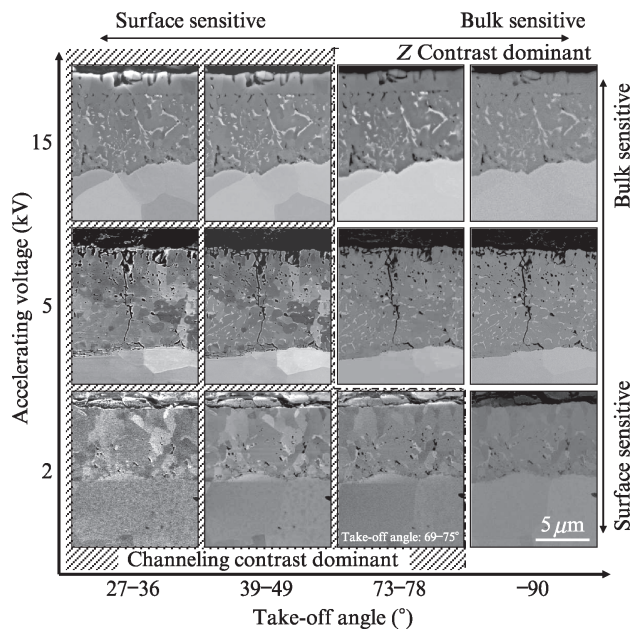
3. Selective Visualization of BSE Information

3.1 Selective Visualization of Mean Atomic Number Information and Crystallographic Information

Backscattered electrons (BSE) originate primary electrons that have penetrated into a specimen and then are reemitted from the specimen surface; their energy range is from a few 10 eV to E_p . Because BSE images represent contrasts caused by the crystal orientation, mean atomic number (Z) and topography of the material, they are widely used in microstructural observation of a variety of materials including steel materials. However, these contrasts are generally observed as superimposed in a BSE image. As in the case of SE, JFE Steel demonstrated selective visualization of this information by appropriately selecting the observation conditions and detectors^{8,9,12,14)}.

The changes in the contrast of BSE images were investigated systematically in the cross section of a low carbon steel specimen, which had been heat-treated to form an oxide layer on the surface, by independently changing E_p and the BSE take-off angle (θ) as seen from the specimen surface^{8,9)}. The results clarified the fact that bulk information and Z contrast increase at high E_p , and surface information and channeling contrast, which is caused by differences in crystal orientation, increase at low E_p . It was also shown that bulk information and Z contrast increase at high θ , and surface information and channeling contrast increase at low θ . These results were summarized in a diagram (**Fig. 1**^{8,9)}) which shows the relationship between SEM observation conditions and contrasts, and has become an index for determining the observation conditions for BSE images. For example, in **Photo 3**^{8,9)}, image (a) emphasizes channeling contrast and image (b) emphasizes Z contrast. These images can be acquired simultaneously by using BSE detectors with different θ at $E_p=5$ keV. It is possible to clarify the shape and distribution of crystal grains of the oxide layer and the base steel from Photo 3 (a). It is also possible to define the interface between the oxide layer and base steel and analyze the size and distribution of fine iron particles dispersed in the oxide layer from Photo 3 (b).

The key point in selective visualization of BSE information is preferential detection of the electrons that contribute to the target information. BSE are composed of low loss electrons (LLE), which lost almost none of the energy of the primary electrons, and an inelastic BSE,



The areas where the mean atomic number (Z) contrast and channeling contrast are enhanced are indicated by shaded and unshaded areas, respectively.

Fig. 1 Schematic diagram showing the take-off angle and accelerating voltage dependencies of the backscattered electron (BSE) contrast of the cross-section of the heat-treated low carbon steel^{8, 9)}

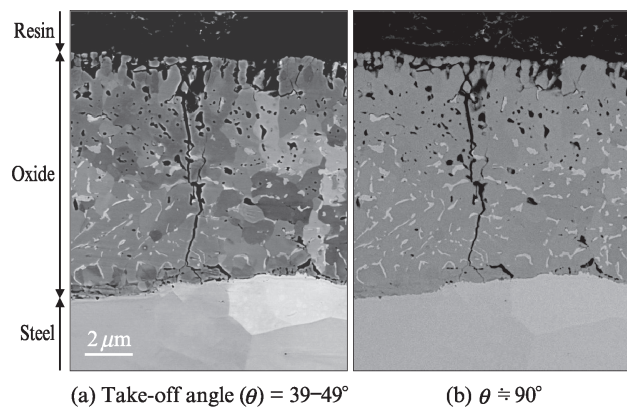


Photo 3 Backscattered electron (BSE) images of the cross section of heat-treated low carbon steel obtained with different take-off angles (θ)^{8, 9)} (The primary energy of incident electron (E_p) was 5 keV from the same area.)

which lost energy. Channeling contrast is mainly caused by the fact that the LLE produces anisotropy corresponding to the crystal orientation¹⁷⁾. On the other hand, Z contrast is due to the dependence of backscattering coefficient on the mean atomic number of the substance, and both the LLE and the inelastic BSE contribute to Z contrast¹⁷⁾. By applying surface-sensitive observation conditions by setting a low θ and low E_p , it is possible to increase the detection ratio of the LLE component, which occurs at the surface from approximately a few nm to a few 10 nm, and thereby emphasize channeling contrast. Conversely, Z contrast can be emphasized by setting high θ and high E_p conditions to reduce the LLE

component detection ratio.

Thus, it is also possible to emphasize surface information corresponding to the purpose of observation in BSE images by selecting appropriate observation conditions and detectors based on the contrast formation mechanism.

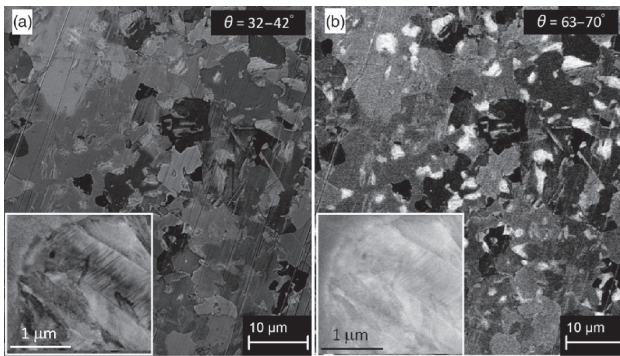
3.2 Visualization of Steel Microstructure

For control of the microstructure of multi-phase steels, it is important to evaluate the phase fraction, such as ferrite (F) and martensite (M) phases, the crystal size and shape, etc. In observation of the microstructure of steel materials, the method of SEM observation of irregularities after polishing the sample, followed by etching with acid or other chemicals or ion irradiation, was widely used. However, with progress in the refinement of the steel microstructure and the adoption of multi-phase materials in recent years, it has become difficult to identify phases and observe microstructures by the conventional method. Observation of these fine, complex microstructures is also possible by techniques for selective detection and visualization of BSE¹³⁾.

Photo 4¹³⁾ shows BSE images of the polished surface of a dual-phase steel consisting of an F phase and M phase, when θ of the BSE detector was changed by controlling the working distance and E_p was constant at $E_p=15$ keV. Under the low θ condition shown in Photo 4 (a), channeling contrast is enhanced, and it is difficult to distinguish phases by contrast; however, fine structures in the M phase, namely, laths and twin structures, can be observed, as shown in the enlarged view of the M phase at the lower left. Under the high θ condition, as shown in Photo 4 (b), it is possible to distinguish the M phase as bright contrast. As a result, selective observation of the M phase is possible, and the size, distribution and fraction of the M phase can be obtained by image analysis.

The fact that the M phase is observed by bright contrast under high E_p and high θ conditions is considered to be because these conditions reduce channeling contrast (see Fig. 1) and emphasize the multiple scattering effect of BSE caused by the high plane defect and dislocation densities in the M phase, where these densities are far higher than those in the F phase¹³⁾. However, since BSE images are bulk sensitive under these conditions, as shown in Fig. 1, the boundaries of the laths and twins in the M phase are indistinct, as can be seen in the enlargement at the lower left of Photo 4 (b).

As described above, it is possible to grasp the microstructure of steel materials in detail, over a wide scale range, by properly selecting the observation conditions and detectors based on an understanding of the contrast formation mechanism. Quantitative analysis of the steel microstructure is also possible, and beneficial knowl-



(a) Take-off angle (θ) = 32–42° (b) θ = 63–70°

The insets are enlarged images of a martensite.

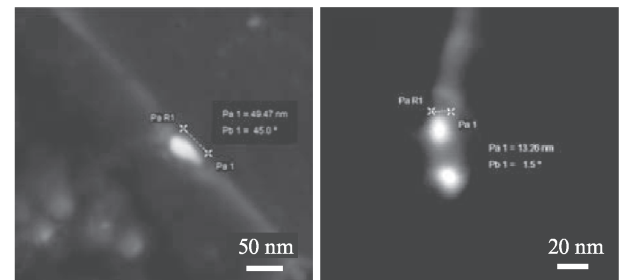
Photo 4 Backscattered electron (BSE) images of a complex phase steel taken at different take-off angles (θ_s) from the same area¹³⁾ (The primary energy of incident electron (E_p) was 15 keV. Kaoru Sato, Hitoshi Sueyoshi and Katsumi Yamada, Characterization of complex phase steel using backscattered electron images with controlled collection angles, *Microscopy*, 2015, Vol. 64, No. 5, 300, by permission of The Japanese Society of Microscopy.)

edge related to improvement of mechanical properties can be obtained.

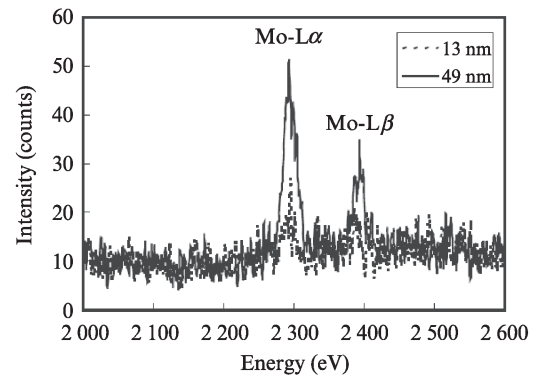
4. Elemental Analysis Techniques Using Low Accelerating Voltage

Elemental analysis of local areas by characteristic X-ray in SEM is normally performed by energy dispersive X-ray spectroscopy (EDS). Observation of topographic and material information on surface region has become possible by low accelerating voltage SEM (LV-SEM, ≤ 5 kV) with high special resolution, although it was difficult under the conventional conditions. On the other hand, because the K lines of the light elements to 3d transition elements are used in SEM-EDS analyses of ferrous materials, measurement have been performed commonly at $E_p \geq 10$ keV. However, under this condition, primary electrons penetrate to a deep region in the specimen, and detection region of the characteristic X-ray becomes the sub-micron order. This can cause differences in the information depth and regions of SEM images observed at low E_p and the results of analysis at high E_p , and in some cases, it is difficult to associate the obtained analytical results and the images acquired by ULV-SEM. To solve this problem, JFE Steel carried out various studies on LV elemental analysis techniques utilizing X-ray spectrometers, including EDS and others^{18–21)}.

Among those studies, this chapter introduces efforts using the Transition Edge Sensor (TES), which offers to measure characteristic X-rays over a comparatively wide energy range with high energy resolution. **Figure 2**¹⁹⁾ shows SE images and the TES spectra of fine carbides in



(a) Secondary electron (SE) image (b) SE image of a 13 nm sized of a 49 nm sized carbide



(c) Mo-L transition edge sensor (TES) spectra

Fig. 2 Secondary electron (SE) images and Mo-L transition edge sensor (TES) spectra of fine carbides in a high strength steel¹⁹⁾ (The primary energy of incident electron (E_p) was 5 keV.)

a high strength steel when measured at $E_p=5$ keV. It was possible to detect Mo contained in the carbides with diameters of 47 nm and 13 nm, which were exposed on the steel surface by electropolishing, thereby demonstrating the possibility of achieving high spatial resolution analysis corresponding to LV-SEM images¹⁹⁾. **Figure 3**¹⁹⁾ shows a BSE image and the TES spectra of the polished cross section of the oxide layer formed on the surface of a hot-rolled steel sheet when measured at $E_p=5$ keV. The area shown by A in Fig. 3 (a) is the substrate steel sheet, the position shown by B in the oxide layer is an Fe particle, the light gray area shown by C is FeO, and the dark gray area shown by D is Fe₃O₄. Focusing on the relative intensity of Lβ to Lα in the Fe-L line spectra shown in Fig. 3 (b), it is possible to distinguish the metallic state and oxide state of Fe based on the fact that the relative intensity of the oxides tends to be high in comparison with the metallic phase¹⁹⁾.

Because LV elemental analysis techniques enables characterization of elemental components near the top-most surface region and their chemical states with high spatial resolution, this is considered to be a useful tool for the development of steel products when used in combination with selective visualization techniques for surface information by SEM.

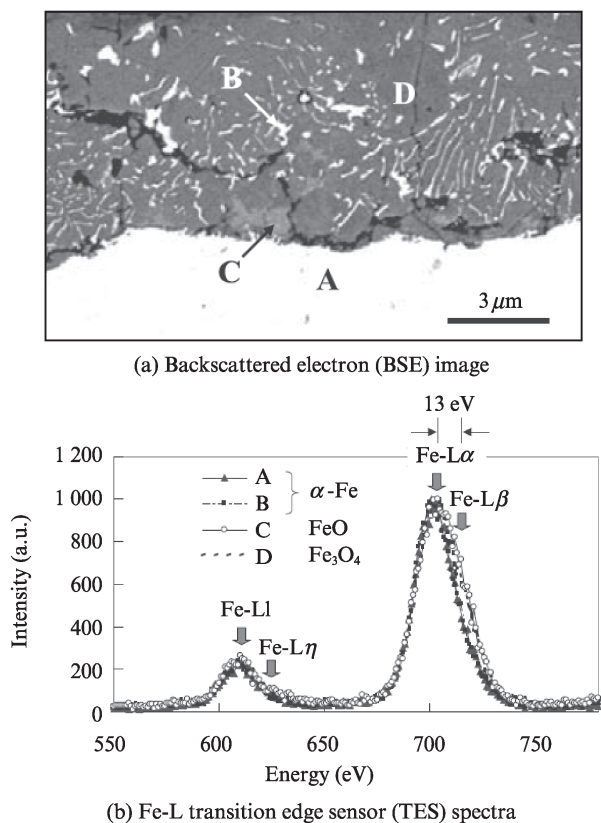


Fig. 3 Backscattered electron (BSE) image and Fe-L transition edge sensor (TES) spectra of cross-section of hot-rolled steel¹⁹⁾ (The primary energy of incident electron (E_p) was 5 keV.)

5. Conclusion

JFE Steel has verified the effects of observation and detection conditions on various types of contrasts by experimental^{10,13,14)} and simulation-based approaches¹⁵⁾, and has applied this knowledge to selective visualization techniques for microstructural information on steel materials.

This report has presented examples of selective visualization of surface information on steel materials by SEM and efforts to realize LV elemental analysis. These techniques offer the following advantages.

- (1) Appropriate selection of SEM observation conditions and detectors enables selective visualization of diverse types of information, namely, the surface material and topography, Z and crystallography.
- (2) By applying the above-mentioned SEM observation techniques, the microstructures of ferrous materials including multi-phase steels can be characterized a wide range of scales.
- (3) LV elemental analysis makes it possible to improve surface sensitivity and spatial resolution. It is also possible to perform chemical state analysis by using an X-ray detector with high energy resolution.

As a result, it has become possible to selectively visualize target information on the surface and fine structures of steel materials, and the microstructure of

steel materials can now be characterized in greater detail.

JFE Steel is now exploring new SEM observation techniques, such as selective visualization of the microstructures of multi-phase steels^{22,23)}, etc., by applying ULV-SEM in which primary electrons are decelerated by giving a negative bias to the specimen. In the future, we will continue to improve SEM observation techniques and their application based on various types of contrast formation mechanisms. We will also work toward a deeper understanding of the relationship between the microstructures and properties of ferrous materials by strengthening interactions between SEM observation and analytical techniques, and will use this knowledge to accelerate the development of new steel materials.

References

- 1) Knoll, M. Z. *Tech. Physik.* 1935, vol. 16, p. 467–475.
- 2) Oatley, C. W. *The Scanning Electron Microscope, Part I. The Instrument.* Cambridge, UK, Cambridge University Press, 1972.
- 3) McMullan, D. *Scanning.* 1995, vol. 17, p. 175–185.
- 4) Nagoshi, M.; Kawano, T.; Sato, K. *J. Surf. Finish. Soc. Jpn.* 2003, vol. 54, p. 31–34.
- 5) Sato, K.; Nagoshi, M.; Kawano, T.; Homma, Y. *Oyo Buturi*, 2004, vol. 73, p. 1328–1332.
- 6) Kawano, T.; Nagoshi, M.; Sato, K. *JFE Giho.* 2006, no. 13, p. 5–8.
- 7) Sato, K.; Nagoshi, M.; Kawano, T. *Tetsu-to-Hagané.* 2007, vol. 93, p. 169–175.
- 8) Aoyama, T.; Nagoshi, M.; Nagano, H.; Sato, K.; Tachibana, S. *Tetsu-to-Hagané.* 2010, vol. 96, p. 654–658.
- 9) Aoyama, T.; Nagoshi, M.; Nagano, H.; Sato, K.; Tachibana, S. *ISIJ Int.* 2011, vol. 51, p. 1487–1491.
- 10) Nagoshi, M.; Aoyama, T.; Sato, K. *Ultramicroscopy.* 2013, vol. 124, p. 20–25.
- 11) Nagoshi, M.; Tanimoto, W.; Higai, K.; Hoshino, K.; Yamasaki, Y.; Kijima, H. *ISIJ Int.* 2014, vol. 54, p. 2854–2859.
- 12) Aoyama, T.; Nagoshi, M.; Sato, K. *Surf. Interface Anal.* 2014, vol. 46, p. 1291–1295.
- 13) Sato, K.; Sueyoshi, H.; Yamada, K. *Microscopy.* 2015, vol. 64, p. 297–304.
- 14) Aoyama, T.; Nagoshi, M.; Sato, K. *Microscopy.* 2015, vol. 64, p. 319–325.
- 15) Tandokoro, K.; Sato, K.; Nagoshi, M.; Tsuno, K. *Abstr. of The 71st Annu. Meet. of The Jpn. Soc. of Microsc.* 14amA_12–07, 2015, p. 57.
- 16) Reprinted from *Ultramicroscopy*, Vol. 124, M. Nagoshi, T. Aoyama, K. Sato, Extraction of topographic and material contrasts on surfaces from SEM images obtained by energy filtering detection with low-energy primary electrons, 23, Copyright (2012), with permission from Elsevier.
- 17) E. g., Reimer, L. *Scanning Electron Microscopy. Physics of Image Formation and Microanalysis.* 2nd Edition. Berlin, Heidelberg, Springer-Verlag, 1998.
- 18) Sato, K.; Noro, H.; Nagoshi, M.; Yamada, K.; Tanaka, K.; Tachibana, S. *Proceedings of the 17th International Microscopy Congress (IMC17).* Rio de Janeiro, Brazil, 2010–09-19/24. International Federation of Societies for Microscopy, 2010, 13–6.
- 19) Noro, S.; Sato, K.; Tanaka, K. *J. Surf. Sci. Soc. Jpn.* 2010, vol. 31, p. 610–615.
- 20) Nagoshi, M.; Sato, K. *CAMP-ISIJ.* 2014, vol. 27, p. 518.
- 21) Nagoshi, M.; Sato, K. *Surf. Interface Anal.* 2014, vol. 46, p. 865–868.
- 22) Mikmeková, Š.; Yamada, K.; Noro, H. *Microscopy.* 2013, vol. 62, p. 589–596.
- 23) Mikmeková, Š.; Yamada, K.; Noro, H. *Microscopy.* 2015, vol. 64, p. 437–443.